

Visualization of the Electrostatic Potential Distribution in Both Polar Ionospheres Using Multiple Satellite Measurements

MARCR. HAIRSTON and RODERICK A. HEELIS
Center for Space Sciences, University of Texas at
Dallas, Richardson, TX

FREDERICK J. RICH
Phillips Laboratory, Geophysics Directorate, Hanscom
AFB, MA

During the time from December 1991 through March 1992, there were four operational DMSP satellites in polar orbit. All four satellites carried the SSIES plasma package which included an ion drift meter. Data from the drift meter, combined with the magnetic field data, allowed the calculation of the electrostatic potential in the ionosphere along the satellite's path. Simultaneous polar coverage by four satellites was unprecedented, providing researchers with almost continuous monitoring of the potential distribution in both hemispheres for the four month period. Combining the magnitude and location of the potential data from each of the four satellites in order to examine the varying potential distribution pattern in both hemispheres presented a major challenge in data visualization. The problem was solved by developing a three-dimensional presentation of the data where the potentials are color coded and represented by the vertical dimension. This paper presents examples from a computer animation of several days of data demonstrating evolution of the size and shape of the potential distribution, along with how these changes correspond to variations in other geophysical parameters, such as the IMF orientation and the K_p index.

1. INTRODUCTION

The National Center for Supercomputing Applications (NCSA) produced video "Numerical Modeling of a Severe Thunderstorm" [Wilhelmson et al., 1989] is perhaps the best known example of the application of computer animation to present a large and complex scientific data set in a clear manner. As such, it sets a standard that many scientists strive to equal in the animated visualizations of their own results. However, most scientists and researchers do not have access to the high-end computers and video resources necessary to produce such impressive animations. This paper will describe a system developed at the Center for Space Sciences at the University of Texas at Dallas for producing high quality stills and animations using relatively inexpensive equipment. More importantly, this paper will also demonstrate how these animations and visualizations are applied to the large data sets used in the analysis of the shape and evolution of the electrostatic potential distribution in the polar regions of the Earth's ionosphere.

2. BACKGROUND

The Center for Space Sciences builds an ion drift meter instrument as part of the Special Sensor-Ions, Electrons, Scintillation (SSIES) package, which flies on the polar-orbiting Air Force weather satellite series (the Defense Meteorological Satellite Program or DMSP) at an altitude of 800 km. This instrument measures the bulk ion velocities in the horizontal and vertical directions perpendicular to the satellite's velocity vector. The ion flows are sampled six times per second for each component and then averaged into four-second bins. As the satellite flies over the polar region, this four-second

ND B

7N-46-CR

43820

resolution flow data is combined with the magnetic field data to calculate the electrostatic potential along the satellite's track. A more detailed description of the analysis techniques used here is given in Hairston and Heelis [1993] and Heelis and Hairston [1990]. The interaction of the interplanetary magnetic field in the solar wind as it moves past the Earth's magnetosphere generates an electric field across the surface of the magnetopause, which in turn produces a potential drop between the dawnside and the duskside. This potential drop is mapped down to the two polar ionospheres producing a potential difference there on the order of tens to hundreds of kilovolts. The exact distribution of the potential across the polar cap region is complicated and has been studied and modeled for the past twenty years [e.g. Heppner and Maynard, 1987; Heelis, 1984; and the references therein]. There is general agreement in these studies that when the interplanetary magnetic field (IMF) in the solar wind is pointed southward (i.e. $B_z < 0$) a region of positive potential forms on the dawnside of the polar region and a corresponding region of negative potential forms on the duskside. The shapes and sizes of these regions vary widely, but are believed to be influenced by the magnitude and sign of the y -component of the IMF. Here the y -axis is oriented parallel to the Earth's orbit with $+y$ directed towards the duskside. When the IMF is oriented northward (i.e. $B_z > 0$), there is less agreement about the nature of the distribution [see Reiff and Burch, 1985] but it is generally accepted that the potential drop is smaller and the overall potential distribution pattern more complicated. While the potential perpendicular to the magnetic field in the polar region covers a two-dimensional area, the data from the satellite only covers a single slice of the pattern as the satellite crosses the pole. Thus, all of the modeling of the potential pattern to date has been based on averaging and binning of data from satellite passes at widely different times [e.g. Rich and Hairston, 1993; Heppner and Maynard, 1987].

The ideal situation would have multiple satellites in orbit simultaneously, each sampling a different region of the pattern. This would insure that a true representation of the global distribution of the potential could be constructed. Such an ideal situation occurred from December 1991 through the end of March 1992, when there were four opera-

tional DMSP satellites in orbit, each in a different local time orientation. This provided an unprecedented opportunity to map the overall electrostatic potential distribution simultaneously in both polar ionospheres and look at short term changes in these patterns. An initial analysis was conducted on a four-day time period from January 26 through January 30, 1992, a time period that also encompassed one of the extended Geospace Environment Modeling (GEM) campaign periods.

3. DESCRIPTION OF THE GRAPHICS

The overall ionospheric potential distribution in one hemisphere can be visualized as a deformed three-dimensional surface over the polar region (Figure 1). Here the magnitude of the potential at a given point is represented by the distance above or below a polar dial. The polar dial denotes the magnetic local times (MLT) and the circles of magnetic latitude down to 50 degrees. In this figure, the positive potential region is shown as the elevated ridge on the right while the negative potential region is shown as the bowl-shaped depression on the left. To further reinforce the distinction between the positive and negative regions, they are also color-coded using grey-white for positive and orange-brown for negative. The potential curve observed by a single satellite pass is presented in the figure as the bright white and orange line along the surface, thus giving a cross-section of the surface along that track. By visualizing the electrostatic potential distribution as this "drumhead" surface, the variations in the potential can be represented as variation in the size and shape of the "drumhead."

Since the potential data are available only along the satellite tracks, three-dimensional plots of the potential curves for all four satellites are overlaid for each hemisphere to form a rough, wireframe representation of the size and shape of the overall potential "drumhead." Figure 2 presents a typical frame from the animation showing an example of the data from both hemispheres during this period. Each frame represents a timestep of twenty minutes centered on the time given in the upper left corner. The northern and southern polar dials are presented as flat surfaces observed from the nightside looking towards the dayside. The polar dials show the most

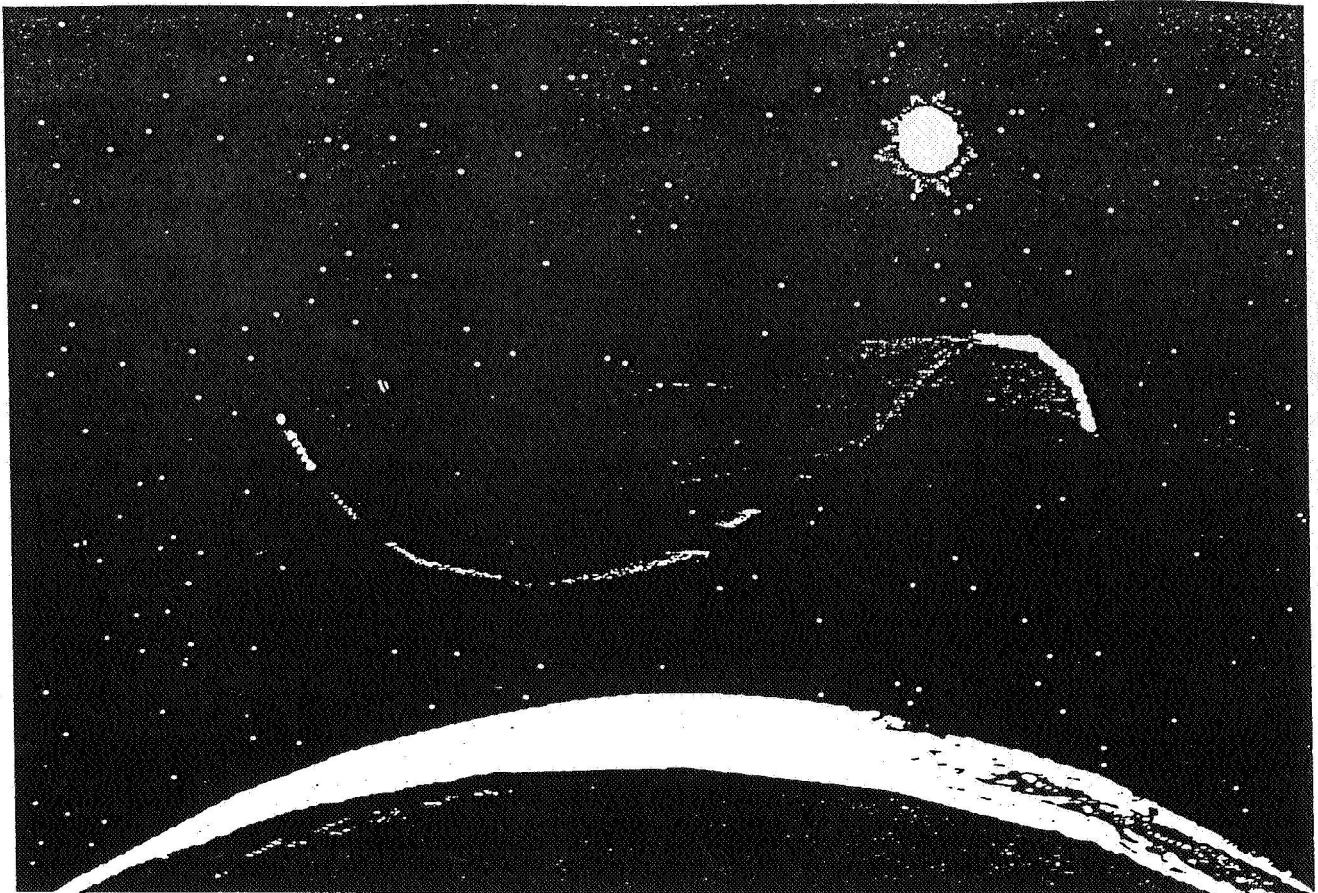


Figure 1. This view shows the northern polar region of the Earth as seen from the nightside. The blue polar dial represents the magnetic latitude in increments of 10 degrees and the crosshair represents the magnetic local times of midnight, 6 am, noon, and 6 pm. The translucent surface represents the electrostatic potential distribution in the northern polar ionosphere with the magnitude of the potential at any point corresponding to the distance above or below the polar dial. Thus, the positive potential region forms a grey-white ridge on the dawnside and the negative potential region forms an orange-brown bowl-shaped depression on the duskside. A sample potential curve that would be observed by a single satellite pass is represented as the bright curve across the surface.

recent passes in each hemisphere for all four satellites. Since the orbital periods of all four satellites are around 105 minutes, this means the pattern in each hemisphere is composed of passes of differing ages. In order to differentiate between the most recent passes and the older passes, the potential curves are color-coded [Tuft, 1990]. A new pass is one in which the satellite reached its highest magnetic latitude during the twenty-minute period of the current frame, and is colored the brightest. A pass that occurred before the current frame, but within the past hour is given a medium color, and any pass more than one hour is shown in the darkest colors. Thus, in the animation the potential curve for a given pass in a given hemisphere will be bright when it first appears, fade to a

medium value for the next two frames, then fade to a dark tone for another two or three frames before it is replaced by the curve from that satellite's next polar pass in that hemisphere. The observed maximum and minimum potential on each satellite's pass are represented by vertical red lines between the curve and the polar dial. For times of southward IMF, these vertical lines roughly denote the polar cap boundary on each polar dial. In the lower left corner of the frame is a plot of the K_p index during the four-day period of this data set with a vertical bar marking the current time.

In the northern hemisphere in Figure 2, the four potential curves suggest a surface with a large dome-shaped positive potential region that extends from the dawnside past the noon-midnight line and

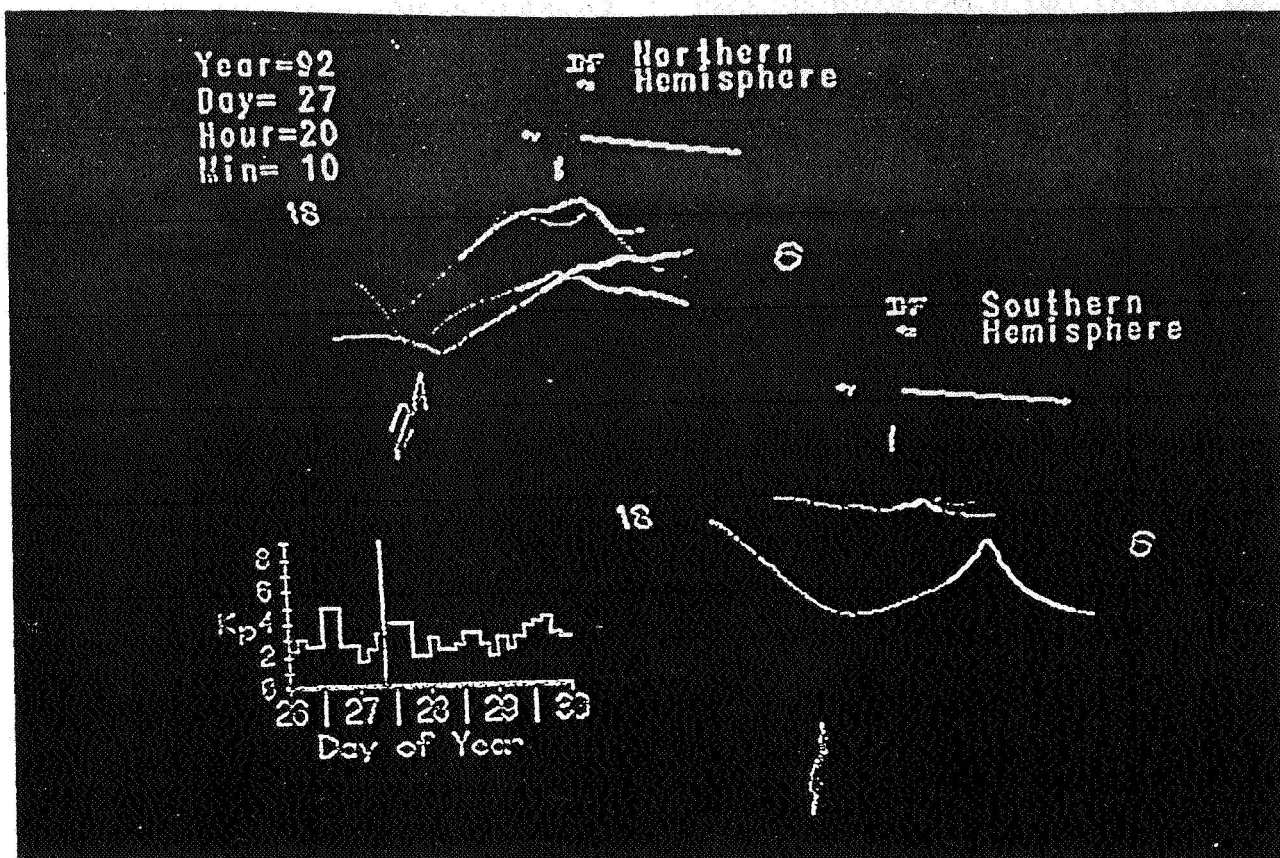


Figure 2. This is a typical frame from the animation showing the potential curves observed by the satellites in both hemispheres presented on polar dial graphs indicating the magnetic local times (MLT) and magnetic latitudes. Note how the curves mesh together to form a wireframe model of the surface describing the overall potential distribution. New passes that occurred during the 20 minute period represented by this frame are shown in brightest colors. Previous passes less than one hour old are shown in medium colors and passes more than an hour old are shown in dark colors. The vertical red bars indicate the location and magnitude of the maximum and minimum potentials observed along each pass. In the northern hemisphere the largest maximum bar represents 38.8 kV at 5.7 MLT and 76.9 degrees magnetic latitude, while the largest minimum bar represents -61.6 kV at 21 MLT and 69.1 degrees magnetic latitude. The yellow arrows on the crosshairs on the dayside of the polar dials represent the averaged magnitude and orientation of the IMF in the y-z plane during the time period for this frame. Here $B_y = -18.2$ nT and $B_z = -0.8$ nT. In the bottom left corner is a graph showing the K_p index for this study period with a vertical bar indicating the current time.

partway into the duskside. The negative potential region is shaped like a valley and confined to the duskside. The fact that the different colored curves merge to give a coherent shape indicates that this potential distribution had been steady for some time. This distribution is consistent with the observed distribution during times when the IMF B_z is weakly negative (southward) and B_y is strongly negative [Rich and Hairston, 1993; Heppner and Maynard, 1987]. At these times the ion convection pattern in the northern hemisphere is dominated by a large dawn cell. The averaged IMF orientation and magnitude in the y-z plane for this twenty minute period is given as an arrow in the crosshair on the dayside of the polar dials. Note that the

orientation of the crosshair is what an observer would see if looking towards the sun (i.e. +z is upward and +y is to the left). There is a time lag of about 36 minutes between the time the IMF was observed in the solar wind by the IMP-J satellite and the time it is displayed on the crosshair. This time lag corresponds to six minutes for the solar wind transit time between the IMP-J satellite and the nose of the Earth's magnetopause, plus a 30 minute delay for the entire polar ionosphere to respond to the IMF. This 30 minute response time of the ionosphere was determined empirically using this four-day data set.

In the southern hemisphere in Figure 2, the pattern formed by the three potential curves is quite

different. (The fourth curve in the 1400-1600 MLT region is flat showing that this satellite pass did not enter the auroral region.) Here the positive potential region is shaped like a ridge that forms a crescent shape on the dawnside while the negative potential region forms a large bowl-shaped basin extending from the duskside into the dawnside.

This is also consistent with the observed potential distribution in the southern hemisphere during the times when the IMF is predominantly oriented in the $-y$ direction and a large dusk cell dominates the ion convection pattern [Rich and Hairston, 1993; Heppner and Maynard, 1987]. Having multiple satellites providing simultaneous observations in both polar ionospheres clearly demonstrates that the potential distributions in both hemispheres are not mirror images of each other. It should be noted that the orientation of both the northern and southern hemispheric polar dials in Figure 2 match the

orientation seen in Figure 1 (dusk on the left, dawn on the right). This orientation was chosen to emphasize the comparisons between each side of the pattern and its counterpart in the other hemisphere.

4. ANALYSIS

Once all the frames were generated for this study period, they were connected together on the computer so they could be played in sequence as an animation. This proved to be an effective means of presenting the four days of data from four satellites in two hemispheres along with the IMF and K_p data in a form that was clear and understandable to the investigator. The interactive nature of the animations allowed the investigator to "play" the data at variable rates, to stop and examine a single frame at length, or even move backwards through the data. This animation presented the evolution of the

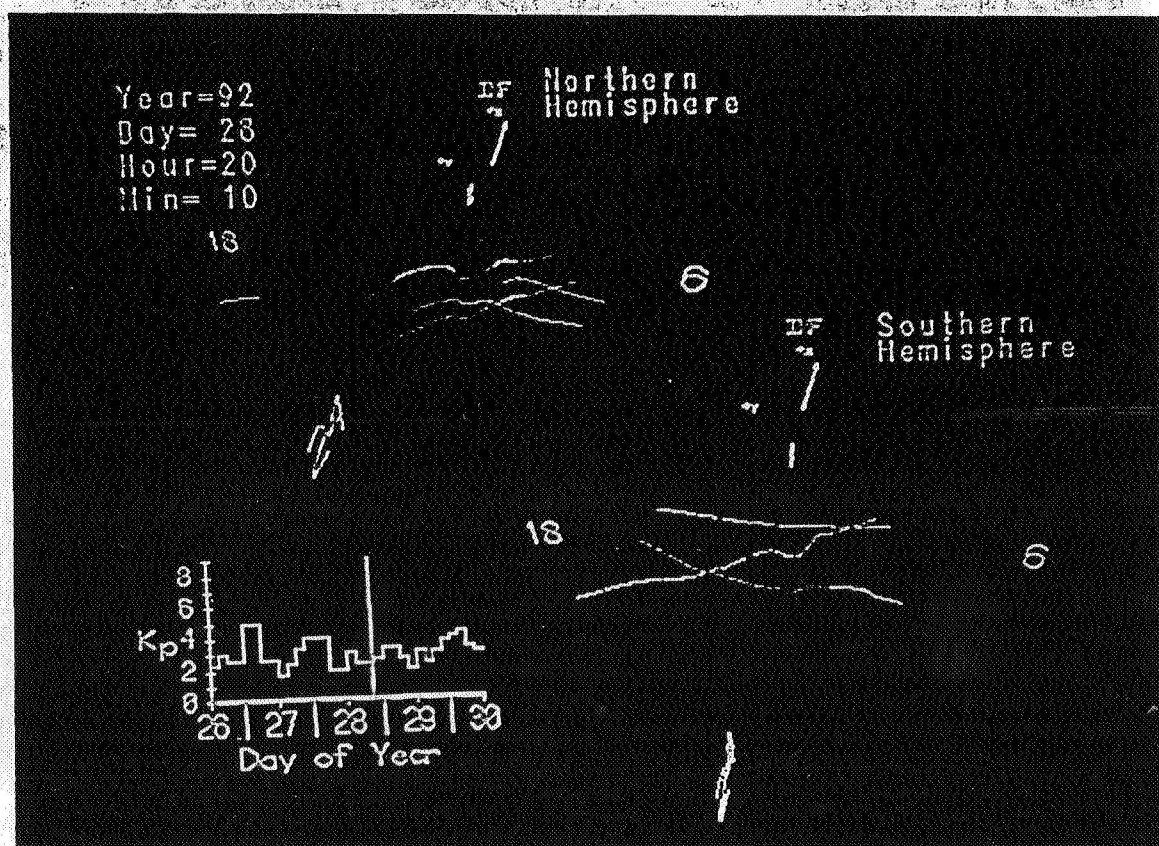


Figure 3. This frame presents a typical distribution seen when the B_z component of the IMF had been strongly positive (northward) for over an hour. During this twenty-minute period the averaged component values were $B_y = -1.5 \text{ nT}$ and $B_z = +4.9 \text{ nT}$. Notice that the overall distribution is no longer organized into the two-cell pattern seen in Figure 2. The surface described by these curves is much flatter than in Figure 2 indicating that the electrostatic potential differences are much smaller.

potential distributions in both hemispheres over time and demonstrated periods of both extended stability and rapid change. This animation was recorded onto videotape for presentation at the spring 1993 AGU meeting (see note at the end of the article). This data set provided a wealth of information that is still being analyzed about the behavior of the ionosphere in response to the IMF.

In this short report, only four cases from the four day study period will be presented. Figure 3 shows a typical pattern observed when the IMF orientation is predominantly B_z positive (northward IMF). The overall potential drop between the dawnside and duskside is much smaller than when B_z is negative (southward IMF), thus causing the surface to appear much flatter than it did in Figure 2. Also, each of the potential curves shows

multiple oscillations rather than the simple sine wave curve seen in the curves in Figure 2. Taken together the curves indicate that the overall distribution is complex in shape and less organized than during times of southward IMF. This distribution is consistent with other observations during times of strongly northward IMF [Cumminock et al., 1992; Heppner and Maynard, 1987]. During conditions of northward IMF there is little or no reconnection between the Earth's magnetic field and the IMF, which accounts for the small potential drop between the dawn and duskside. The large scale two-cell convection pattern seen during southward IMF becomes distorted or breaks up into multiple smaller cells during extended periods of northward IMF. A satellite crossing through these multiple or distorted cells sees multiple reversals in the direc-

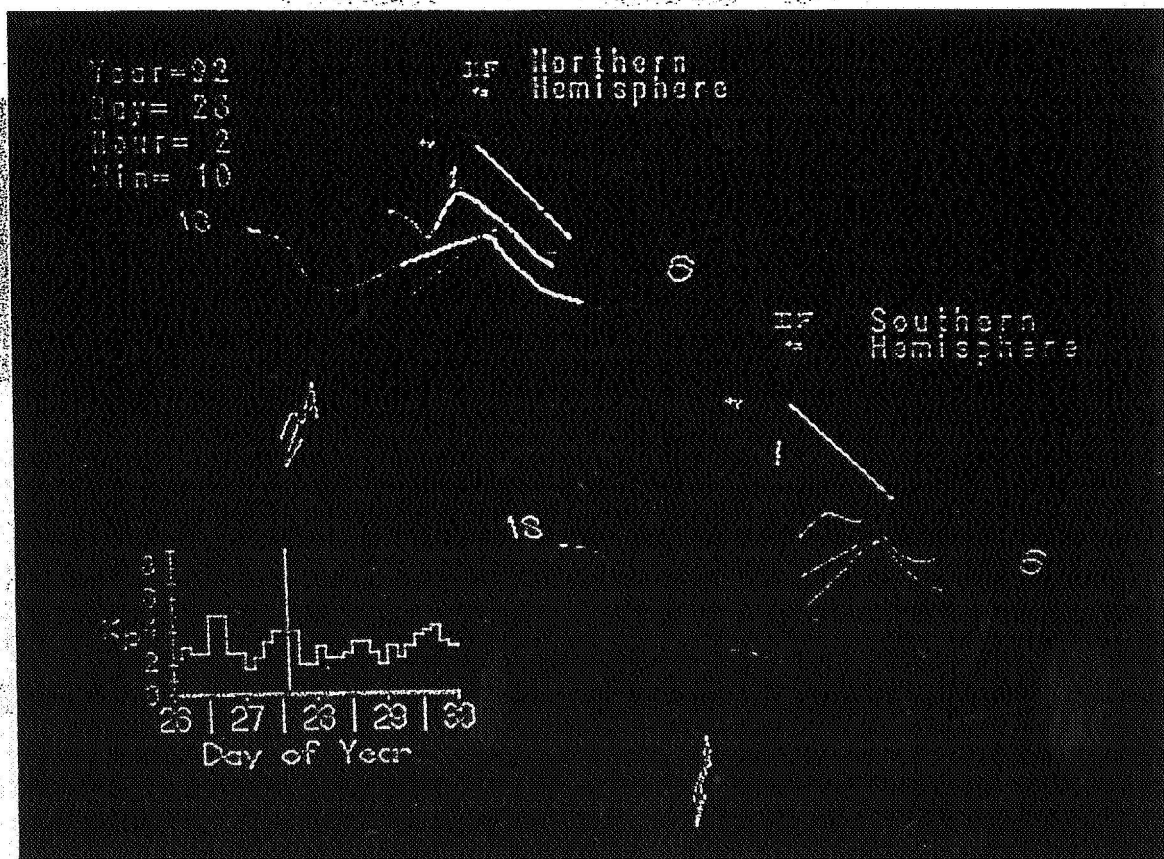


Figure 4. This frame presents a typical distribution when both B_y and B_z are negative and roughly equal in magnitude. During the twenty minutes of this frame the averaged IMF components were $B_y = -12.4$ nT and $B_z = -10.4$ nT. While the distribution is similar in overall form to the one in Figure 2, the rotation of the IMF towards the south changes the sizes of the potential regions. The northern positive potential region contracts back to the noon-midnight line compared to Figure 2, and the southern positive potential region increases in width. In the northern hemisphere the largest maximum bar represents 48.2 kV at 10.2 MLT and 75.9 degrees (magnetic latitude), while the largest minimum bar represents -62.1 kV at 19.3 MLT and 68.0 degrees.

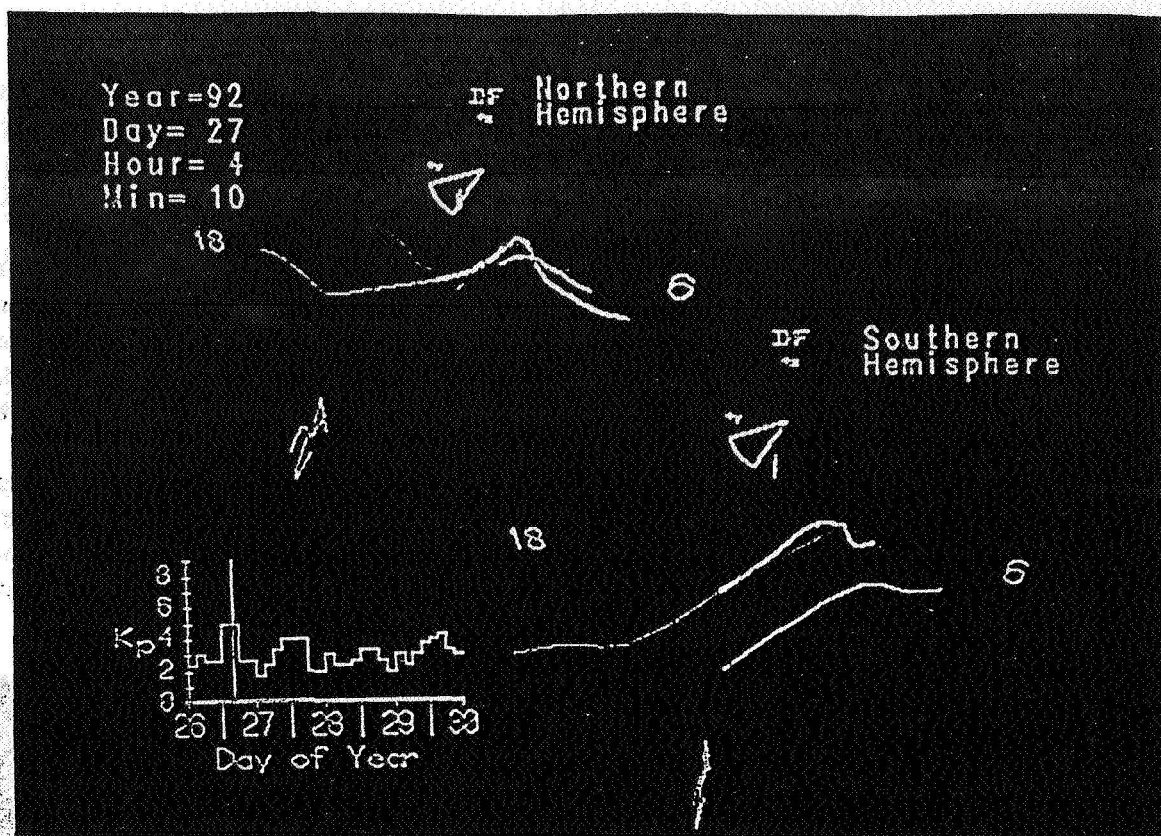


Figure 5. There were no available IMF data during the study period which showed the IMF orientation when B_y is positive and B_z is negative. However, this frame, taken from a period of the study when the IMF data were missing, presents a typical distribution pattern that is consistent with other observations when B_y is positive and B_z is negative. The "wedge" on the IMF crosshair indicates an estimate of the orientation of the IMF. During such periods, the positive potential region in the northern hemisphere contracts over towards the dawnside and the positive potential region in the southern hemisphere expands out to past the noon-midnight line. In the southern hemisphere, the largest maximum bar represents 65.6 kV at 4.0 MLT and -74.2 degrees magnetic latitude, while the largest minimum bar represents -47.7 kV at 18.5 MLT and -67.6 degrees magnetic latitude.

tion of the horizontal ion flow during its pass, thus accounting for the multiple oscillations seen in the corresponding potential curve.

During times of predominantly negative B_z (southward IMF), the overall convection pattern becomes organized into two large cells: a dawn cell and a dusk cell. These convection cells correspond to the positive and negative potential regions (respectively) observed in the potential distribution. During times of southward IMF, there is a strong interaction between the Earth's field and the IMF, which drives the ion convection cells in the ionosphere and produces the potential drop between the dawn and duskside. Figure 4 shows the distribution for a frame when B_z and B_y had both been negative for several hours. Notice that the potential distribu-

tions are similar to those described in Figure 2. However, in this case, the magnitude of B_z is roughly the same as B_y , which results in the widening of the crescent-shaped positive potential region in the southern hemisphere relative to Figure 2. Also, there is a corresponding shrinkage of the region of positive potential in the northern hemisphere to where it only reaches to the noon-midnight line [Rich and Hairston, 1993].

During times of southward IMF, it is the direction of the y-component of the IMF that largely determines the shape and extent of the convection cells and the overall shape of the potential distribution. Unfortunately, there were no IMF data available during this study period showing B_z negative and B_y positive. However, Figure 5 shows

a frame from a period without IMF data that corresponds to the distributions seen at other times when B_z was negative and B_y was positive. The positive potential region in the northern hemisphere has now contracted over to the dawnside forming a ridge shape while the negative potential region forms a shallow basin shape. In the southern hemisphere, the positive potential region has expanded past the noon-midnight line into duskside, confining the negative potential to a small region. Notice that the difference between the patterns in the two hemispheres is not as great as in the cases for Figures 2 and 4. This is consistent with the observations in Rich and Hairston [1993] for conditions when $|B_z| > |B_y|$. The wedge shape on the IMF crosshair indicates the absence of any actual IMF data, as well as the estimate that the

IMF orientation is in the negative B_z /positive B_y quadrant.

One effect of examining the data in an animated form is that the time history of the previous passes make changes in the potential distribution particularly easy to identify. Figure 6 presents a frame which shows a dramatic change in the potential distribution as a result of a change in the IMF. In the previous frames, B_z was positive and B_y was strongly negative. The faded passes in the northern hemisphere of this frame show that the positive potential region was weak and somewhat disorganized. The bright pass in the northern hemisphere is the only new pass to appear during this twenty minute period after B_z turned sharply negative. This new potential curve clearly shows that the positive region had increased in size and

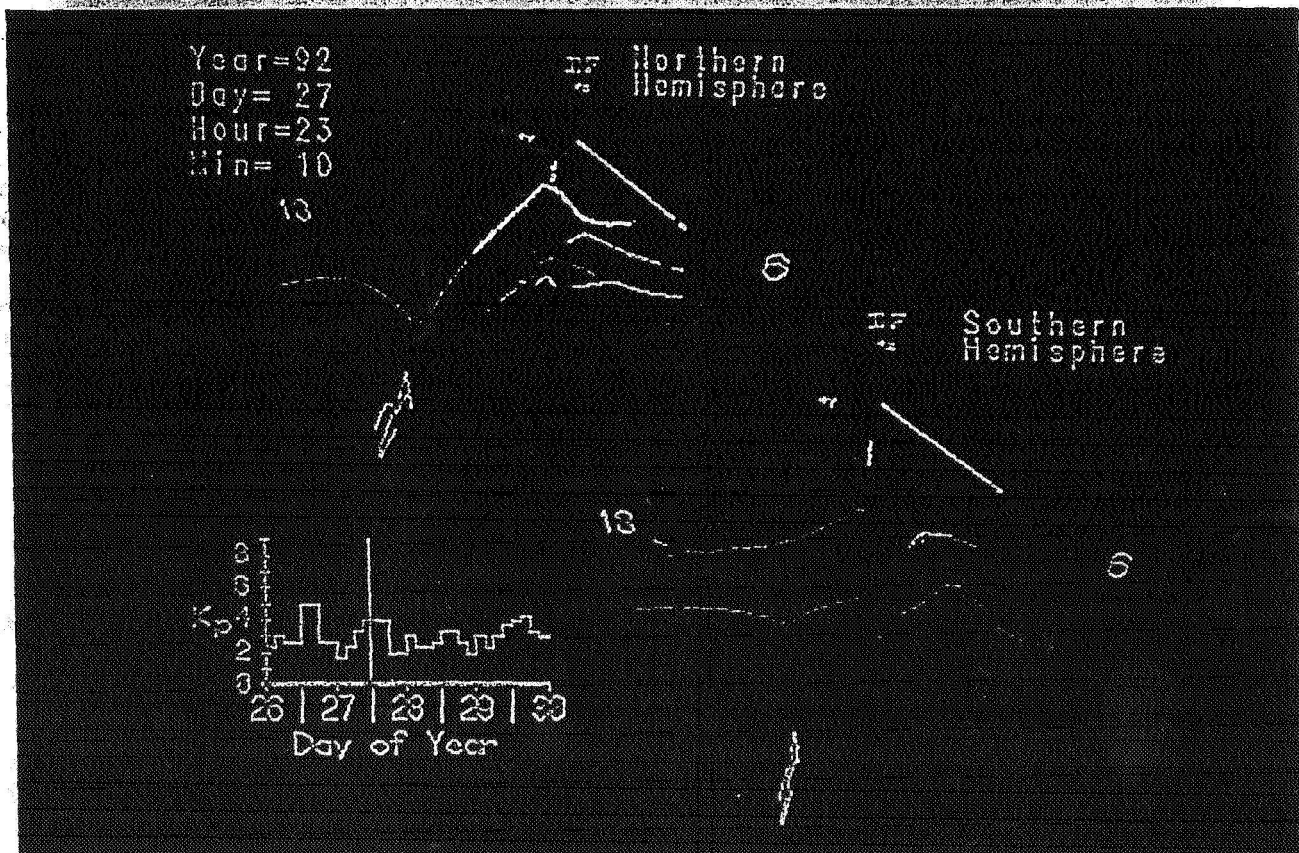


Figure 6. This frame demonstrates using the animation to identify changes in the potential distribution. The dimmed curves in the northern hemisphere are flat and disorganized in the positive potential region, while the negative potential region remains relatively deep and organized. This is indicative of the IMF orientation having a large negative B_y component and a large positive (northward) B_z component. During the previous twenty minute time period prior to this frame the averaged component values were $B_y = -8.7$ nT and $B_z = +6.3$ nT. However, the B_z component turned negative (southward) at the end of that period and during the current twenty minute period of this frame, the averaged component values have changed to $B_y = -14.4$ nT and $B_z = -9.3$ nT. The new potential curve that appears during this frame in the northern hemisphere shows the dramatic change in the size and shape of the potential distribution pattern.

strength compared to the previous potential curves in the northern hemisphere. Such events were used to quantify the response time of the ionosphere to various changes in the IMF as mentioned in section 3.

5. PRODUCTION OF THE ANIMATION

The animation and figures were produced using a VAX 4000 VLC workstation in conjunction with a Commodore Amiga 3000 personal computer. The processing of the raw telemetry data and the analysis to determine the electrostatic potential data for each pass were performed on the VAX. These processed data were used to generate individual frames in color on the VAX using a Tektronix plotting format. However, there was not an inexpensive way to make the VAX suitable for the playback of these individual frames as an animation. Even if it were possible, there was no inexpensive way to transfer such an animation from the VAX to video. This problem was solved by using the relatively inexpensive Amiga. The Amiga was hooked into the VAX cluster via ethernet and used a public domain terminal emulator called VLT [Weinstein, 1991]. The emulator enabled the Amiga to convert the plots downloaded from the VAX in Tektronix format to the IFF graphics format used by the Amiga. Once all the frames were downloaded and converted on the Amiga, commercially available software was used to string the frames together into an animation. This commercial software also allowed the user to modify the colors used and vary the playback speed of the animation. Since the Amiga was specifically designed as a video/multimedia platform, recording the video was a straightforward process of connecting a genlock (a device that converts the computer's RGB video output to standard NTSC video signal) to the computer, and then videotaping the output.

6. CONCLUSION

We have demonstrated in this paper that it is possible to create effective and useful scientific visualization animations using relatively inexpensive equipment. These animations enable researchers to see quickly and easily the shapes and sizes of the distributions of the electrostatic potential in the

ionosphere. While these images are not comparable to animations produced on high-end systems, the overall quality is still quite high and suits the needs of the researcher. Most of the work done to date in modeling the overall pattern of the electrostatic potential distribution has focused on static patterns which arise during long periods of stable IMF conditions. In reality, the IMF is rarely stable for time periods greater than an hour; thus the potential distribution in the ionosphere is quite variable and does not always match the static models. As researchers begin to model this variability and the time-dependence of the potential distributions, computer animations of the data, such as presented here will become an essential tool of that work.

Note: A copy of the animation of this work (NTSC only) will be sent to anyone who sends the authors a blank VHS videotape (still in the original wrapper) with a self-addressed stamped return envelope. Please mail requests to: Marc Hairston, Center for Space Sciences, University of Texas at Dallas, PO Box 830688 FO22, Richardson TX 75083-0688.

Acknowledgments. The authors wish to thank Dr. Ron Lepping of the NASA Goddard Space Flight Center and Drs. Barbara Emery and Gang Lu of the National Center for Atmospheric Research/High Altitude Observatory for providing the IMF data for this time period. The authors also wish to thank Professor Barry Treu of the Visual Arts Department of the University of Texas at Dallas for his assistance in producing the animation and Dr. Robin Coley of the Center for Space Sciences for his assistance in this work. This work was supported by the Air Force through Phillips Laboratory/Geophysics Directorate under contracts F19628-90-K-0002 and F19628-93-K-0007 and NASA grant NAGW-1665.

REFERENCES

- Cummnock, J.A., R.A. Heelis, and M.R. Hairston, Response of the ionospheric convection pattern to a rotation of the interplanetary magnetic field on January 14, 1988, *J. Geophys. Res.*, 97, 19449-19460, 1992.

- Hairston, M.R., and R.A. Heelis, High-latitude electric field studies using DMSP data, Tech. Rep., PL-TR-93-2036, Phillips Lab./Geophy. Directorate, Hanscom AFB, MA, 1993.
- Heelis, R.A., The effects of interplanetary magnetic field orientation on dayside high-latitude ionospheric convection, *J. Geophys. Res.*, 89, 2873-2880, 1984.
- Heelis, R.A., and M.R. Hairston, Studies of ionospheric dynamics utilizing data from DMSP, Tech. Rep., GL-TR-90-0047(I), Air Force Geophys. Lab., Hanscom AFB, MA, 1990.
- Heppner, J.P., and N.C. Maynard, Empirical high-latitude electric field models, *J. Geophys. Res.*, 92, 4467-4489, 1987.
- Reiff, P.H., and J.L. Burch, IMF B_y -dependent plasma flow and birkeland currents in the dayside magnetosphere, 2., A global model for northward and southward IMF, *J. Geophys. Res.*, 90, 1595-1609, 1985.
- Rich, F.J., and M. Hairston, Large-scale convection patterns observed by DMSP, *J. Geophys. Res.*, in press, 1993.
- Tufte, E.R., *Envisioning Information*, Graphic Press, Cheshire Connecticut, 1990.
- Weinstein, A., *A Valiant Little Terminal: A VLT User's Manual*, 121 pp., Stanford Linear Accelerator document SLAC-370 (Rev. #3), July 1991.
- Wilhelmson, R., H. Brooks, B. Jewett, C. Shaw, L. Wicker, "Study of a Numerically Modeled Severe Storm," video by the National Center for Supercomputing Applications, 1989.